Redox Biology 14 (2018) 509–521

Contents lists available at ScienceDirect

Redox Biology

journal homepage: www.elsevier.com/locate/redox

Research paper

Glutaredoxin-2 controls cardiac mitochondrial dynamics and energetics in mice, and protects against human cardiac pathologies

Georges N. Kanaan[a], Bianca Ichim[a], Lara Gharibeh[a], Wael Maharsy[a], David A. Patten[a], Jian Ying Xuan[a], Arkadiy Reunov[b], Philip Marshall[c], John Veinot[b,d,e], Keir Menzies[a,c], Mona Nemer[a], Mary-Ellen Harper[a,*]

[a] Department of Biochemistry, Microbiology and Immunology, and Ottawa Institute of Systems Biology, Faculty of Medicine, 451 Smyth Road, Ottawa, ON, Canada K1H 8M5
[b] Ottawa Heart Institute, University of Ottawa, 40 Ruskin Street, Ottawa, ON, Canada K1Y 4W7
[c] Interdisciplinary School of Health Sciences, University of Ottawa, Faculty of Health Sciences, 451 Smyth Road, Ottawa, ON, Canada K1H 8M5
[d] The Ottawa Hospital, 501 Smyth Road, Ottawa, ON, Canada K1H8L6
[e] Department of Pathology and Laboratory Medicine, and University of Ottawa, Faculty of Medicine, 451 Smyth Road, Ottawa, ON, Canada K1H 8M5

ARTICLE INFO

Keywords:
Human heart
Mitochondria
Oxidative stress
Redox
Cardiac metabolism
Cardiac hypertrophy

ABSTRACT

Glutaredoxin 2 (GRX2), a mitochondrial glutathione-dependent oxidoreductase, is central to glutathione homeostasis and mitochondrial redox, which is crucial in highly metabolic tissues like the heart. Previous research showed that absence of Grx2, leads to impaired mitochondrial complex I function, hypertension and cardiac hypertrophy in mice but the impact on mitochondrial structure and function in intact cardiomyocytes and in humans has not been explored. We hypothesized that Grx2 controls cardiac mitochondrial dynamics and function in cellular and mouse models, and that low expression is associated with human cardiac dysfunction. Here we show that Grx2 absence impairs mitochondrial fusion, ultrastructure and energetics in primary cardiomyocytes and cardiac tissue. Moreover, provision of the glutathione precursor, N-acetylcysteine (NAC) to *Grx2-/-* mice did not restore glutathione redox or prevent impairments. Using genetic and histopathological data from the human Genotype-Tissue Expression consortium we demonstrate that low *GRX2* is associated with fibrosis, hypertrophy, and infarct in the left ventricle. Altogether, GRX2 is important in the control of cardiac mitochondrial structure and function, and protects against human cardiac pathologies.

1. Introduction

Disordered cellular redox underlies the development of many chronic diseases and fundamental processes of aging. Cellular redox balance is maintained through the coordinated regulation of oxidation and reduction processes, and, in turn, plays essential roles in the control of fuel oxidation processes and oxidative stress [1]. During mitochondrial oxidative phosphorylation process, reactive oxygen species (ROS) and reactive nitrogen species (RNS) can overwhelm the antioxidant systems and cause oxidative stress [2,19]. While excessive reactive species levels are detrimental, low levels play key roles in processes such as cellular signaling and protection against infectious agents [3–5]. Within the battery of cellular antioxidant systems, glutathione, which is central to redox homeostasis, is thought to be the most important non-protein antioxidant within cells [6,7,19].

The glutaredoxin (GRX) enzymes are glutathione-dependent oxidoreductases and can protect proteins from oxidative damage [9,10]. Glutaredoxin 2 (Grx2) is expressed in mitochondria of many cell types including cardiomyocytes [14]. We and others previously demonstrated that *Grx2-/-* mice exhibit fibrotic cardiac hypertrophy, hypertension and early onset age-dependent cataract formation [11,42]. However, until now Grx2 implications for human cardiac diseases have been unaddressed. With regard to underlying mechanisms, previous work in isolated cardiac mitochondria, showed that the absence of Grx2 was associated with impaired mitochondrial complex I activity [11]. However, no studies, to-date have assessed the impact of Grx2 deletion at the levels of the intact cell and tissue. Since it is now widely recognised that mitochondria exist in dynamic reticular structures in cells, analyses

Abbreviations: E/A, early filling wave peak (E) and atrial contraction wave peak (A); ECAR, extra cellular acidification rate; EF, ejection fraction; Grx, glutaredoxin; IVS, intraventricular septum; LV, left ventricle; LVID, left ventricular internal dimension; LVPW, left ventricular posterior wall; NAC, N-acetylcysteine; OCR, oxygen consumption rate; PFA, paraformaldehyde; RNS, reactive nitrogen species; ROS, reactive oxygen species

* Correspondence author.
E-mail address: mharper@uottawa.ca (M.-E. Harper).

http://dx.doi.org/10.1016/j.redox.2017.10.019
Received 23 October 2017; Accepted 25 October 2017
Available online 26 October 2017

of mitochondrial function should be conducted, as much as possible, in intact cells and tissues.

Indeed, recent research has demonstrated that mitochondrial fusion is controlled by glutathione redox; specifically, increased levels of oxidized glutathione were shown to increase mitochondrial fusion [8,33]. Our previous work showed high levels of oxidized glutathione in isolated mitochondria from the ventricular cardiac muscle [11] but the repercussions for mitochondrial fusion and ultrastructure remained unknown. Furthermore, the possible implications of glutathione redox for mitochondrial fusion in non-transformed cells and *in vivo* have not been elucidated. Thus the overall aims of this research were to address: (1) the impact of Grx2 deficiency on mitochondrial structure and function in intact cellular systems, (2) the effect of *in vivo* supplementation of the glutathione precursor, N-acetylcysteine (NAC) [34], and (3) the role of GRX2 in human heart in association with cardiac pathologies.

Here we report that GRX2 absence results in disordered cardiac mitochondrial ultrastructure, a hyperfused mitochondrial reticulum and impaired oxidative and glycolytic capacities that are not reversed by NAC. The *in vivo* functional and structural abnormalities, cardiac hypertrophy, fibrosis and hypertension cannot be resolved by NAC treatment. Finally, using publically available datasets from the human Genotype-Tissue Expression (GTEx) consortium, we demonstrate for the first time in humans that low levels of *GRX2* transcripts are associated with fibrosis, hypertrophy, and infarct in the left ventricle, thus demonstrating that this mitochondrial oxidoreductase is essential for heart health.

2. Results

2.1. Grx2-/- male mice develop cardiac hypertrophy and diastolic dysfunction that NAC fails to reverse

To address our first aim, we conducted *in vivo* analyses of heart and *ex vivo* high resolution respirometry in permeabilized cardiac myofibers, in which mitochondria remain in reticular structures. We also queried whether NAC would prevent any dysfunction. Thus, half of all *Grx2-/-* and WT mice were treated with NAC for 6 weeks prior to the *ex vivo* cardiac myofiber analyses, which were conducted at 12 weeks of age. *In vivo* echocardiography and hypertension determinations were conducted at 9 and 10 weeks of age, respectively. No difference in water consumption between the groups was observed (data not shown). Results from echocardiography revealed that interventricular septum (IVS) length was increased in *Grx2-/-* mice during systole and diastole compared to WT mice; surprisingly NAC treatment had no effect in *Grx2-/-* or WT mice (Fig. 1A). There was no difference in the left ventricular internal dimension (LVID) length in both systole and diastole (Fig. 1B). The left ventricular posterior wall (LVPW) thickness was increased in systole but not in diastole (Fig. 1C). Even with NAC treatment, left ventricle (LV) mass was still elevated in *Grx2-/-* mice (Fig. 1D). Thus cardiac hypertrophy in *Grx2-/-* mice was not prevented by *in vivo* NAC treatment.

To further investigate cardiac function, we examined cardiac ejection fraction (EF), an indicator of the blood fraction ejected by the left ventricle during systole, and found no significant differences between groups (Fig. 1E), consistent with the conclusion that left ventricle function was not affected. Then, the velocity ratio of the early filling wave peak (E), the atrial contraction wave peak (A) and the E/A ratio were determined. E/A provides a proxy measure of mitral valve function. Given that E/A was lower in NAC treated *Grx2-/- vs* WT mice, with no differences in the untreated groups (Fig. 1F), our results show that NAC treatment induces a mitral valve abnormality in *Grx2-/-* mice. Representative echocardiographic left ventricle images are shown in Supplementary Fig. 1.

2.2. NAC treatment does not mitigate hypertension in Grx2-/- mice

We next determined if *in vivo* NAC treatment would alleviate the hypertension that develops in *Grx2-/-* mice. It is well known that left ventricular hypertrophy can be caused by hemodynamic instability [12]. We found that the hypertension in untreated *Grx2-/-* mice was not diminished by NAC treatment (Fig. 1G). In *Grx2 -/-* mice treated with NAC, diastolic blood pressure was significantly higher than that in NAC treated WT mice; there were no differences in untreated groups (Fig. 1G). These findings are again consistent with detrimental effects of NAC treatment in the absence of GRX2.

2.3. Dysfunctional cardiac myofiber energetics in Grx2-/- mice

Given our previous finding that deficiency of Grx2 leads to dysfunctional energetics in isolated cardiac mitochondria [11,15], we sought to more comprehensively examine metabolic characteristics in cardiac myofibers in which mitochondria remain intact. We also tested the hypothesis that *in vivo* NAC supplementation restores cardiac myofiber energetics in *Grx2-/-* mice. High resolution respirometry of left ventricular myofibers showed significantly lower complex I -driven phosphorylating respiration in NAC treated *Grx2-/-* mice compared to treated WT, but no difference between the untreated groups (Fig. 2A). For complex I and II -driven respiration (maximal phosphorylating respiration), a significant decrease was noted between the untreated groups (genotype effect), but this was no longer apparent in the treated groups (Fig. 2A). This was not due to a rescue of respiration in *Grx2-/-* mice by NAC but due to lower respiration in the WT mice, indicative of an inhibitory effect of NAC on respiratory capacity (Fig. 2A). There was no difference in leak respiration or complex IV activity (Fig. 2A). To test whether the impaired respiration was due to protein oxidation and glutathionylation, we then examined the effect of dithiotheitol (DTT), a powerful reducing agent. We hypothesized that it would abolish the differences in respiration between the groups if the above described effects were due to oxidation or glutathionylation. Findings showed that DTT increased maximal respiration and had no effects on leak or complex IV activities (Fig. 2B), thereby confirming our hypothesis. Altogether, results in intact cardiac myofibers and primary cardiomyocytes show that *Grx2-/-* causes dysfunctional cellular energetics that cannot be prevented by NAC.

2.4. In vivo NAC treatment does not prevent cardiac hypertrophy and fibrosis

Heart weight (normalized to body weight) of untreated *Grx2-/-* mice at 12 weeks of age was 23% greater than untreated WT control mice. NAC treatment failed to prevent the cardiac hypertrophy (Fig. 3A). There were no differences in body weights and, apart from the cardiac hypertrophy, there were no differences in tissue weights between the groups (data not shown). There was a strong trend for left ventricular fibrosis in the hearts of *Grx2-/-* as observed in our previous study ($p = 0.06$) [11]. Surprisingly, NAC treatment resulted in increased fibrosis in *Grx2-/-* mice compared to WT (Fig. 3B–F).

2.5. NAC treatment increases GSSG and lowers glutathione redox in the liver with no effects in the heart of Grx2-/- mice

We next determined if *Grx2-/-* and the *in vivo* NAC treatment affected cardiac muscle glutathione redox potential. In homogenates of left ventricular tissue, there were no significant genotype or treatment differences in reduced (GSH) or oxidized (GSSG) glutathione levels, or their ratio (GSH:GSSG), in the heart (Fig. 4A–C). Thus impaired (oxidized) glutathione redox in the hearts of *Grx2-/-* mice exists only at the mitochondrial level [11]. Given that our *in vivo* NAC treatments did not increase heart tissue glutathione levels, even in WT mice, we then queried whether levels increased in the livers of mice. HPLC

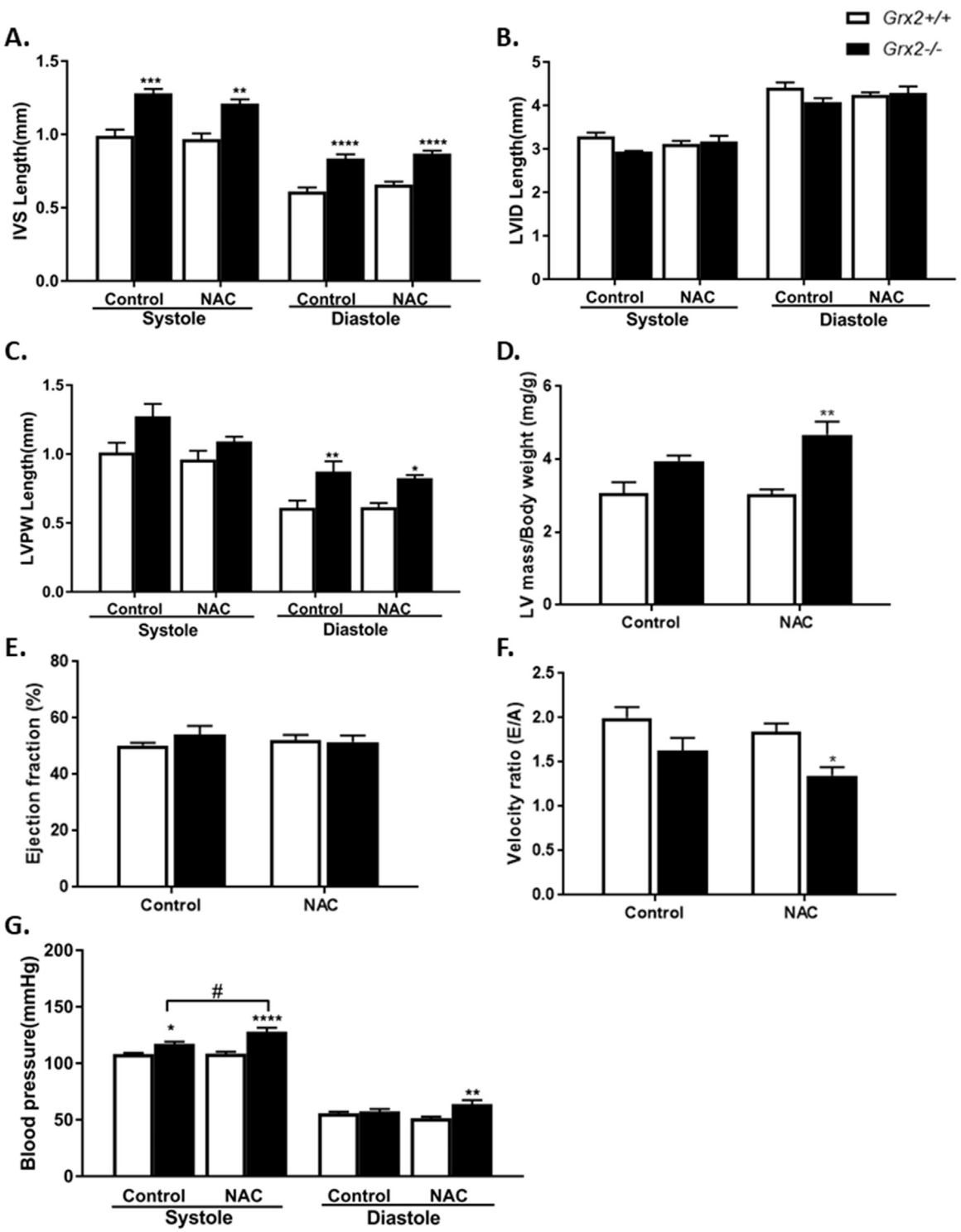

Fig. 1. *Echocardiographic and blood pressure analyses of untreated and NAC treated male mice.* (A–F) Echocardiographic measurements. All mice were 9 weeks of age and measurements were performed on M-mode images. N = 4–5, data are represented as mean ± SEM. Two-way ANOVA with Tukey post-hoc test. *$p < 0.05$, **$p < 0.01$, ***$p < 0.001$, ****$p < 0.0001$. **LV;** Left ventricle, **IVS;** interventricular septum, **LVID;** left ventricular internal dimension, **LVPW;** left ventricular posterior wall. (G) Blood pressure determinations during systole and diastole. N = 6, data are represented as mean ± SEM. Two-way ANOVA with Bonferroni post-hoc test; *$p < 0.05$, **$p < 0.01$, ***$p < 0.001$.

determinations of liver homogenate demonstrated that NAC caused increased GSSG levels, decreased GSH:GSSG, and no change in GSH levels in NAC treated *Grx2-/-* compared to all other conditions (Fig. 4D–F).

2.6. NAC partially restores abnormal mitochondrial ultrastructure in cardiac tissue. A hyperfused mitochondrial network in Grx2-/- cardiomyocytes is unchanged by NAC treatment

Based on the findings of Shutt et al. [8] who demonstrated in HeLa cells that a decrease in glutathione redox causes mitochondrial fusion, and our previous findings of decreased glutathione redox in isolated

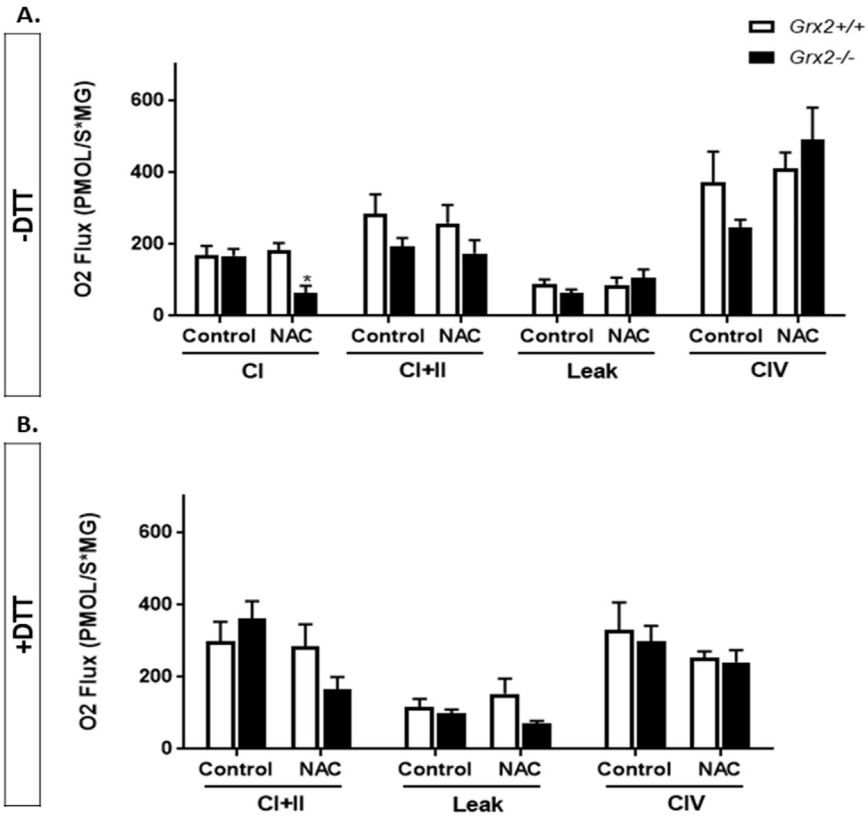

Fig. 2. *Impaired respiration in Grx2-/- intact cardiac myofibers isolated from the left ventricle tissue.* Myofibers were either treated with DTT (B) or not (A). Complex I respiration, complex I+II respiration, leak respiration, complex IV activity were determined. N = 6, data are represented as mean ± SEM. Two-way ANOVA with Tukey post-hoc test; *$p < 0.05$.

mitochondria of *Grx2-/-* hearts [11], we hypothesized abnormal mitochondrial morphology in hearts of *Grx2-/-* mice. Transmission electron microscopic analysis of cross sections of the left ventricle revealed irregular mitochondrial shapes, despite normal cristae density, in untreated *Grx2-/-* mice (Fig. 5B and C) compared to untreated WT mice (Fig. 5A). While 6 weeks of NAC treatment had no effect on WT mitochondria (Fig. 5D), the abnormal morphology of *Grx2-/-* mitochondria were no longer apparent after NAC treatment (Fig. 5E and J).

Next we wanted to investigate the impact of Grx2 and NAC treatment on mitochondrial dynamics. We isolated and studied neonatal cardiomyocytes from *Grx2-/-* and WT mice, and then used immunocytochemistry and quantitative morphometry to assess mitochondrial length. Mitochondria in the *Grx2-/-* cells were hyperfused, with fewer punctate mitochondria than controls (Fig. 5H). There were significantly longer mitochondria in both untreated and in NAC treated *Grx2-/-* cells, thus demonstrating that NAC has no effect on mitochondrial length under these conditions (Fig. 5F–I and K).

2.7. Impaired cellular energetics and metabolic flexibility in Grx2-/- primary cardiomyocytes

We then investigated oxidative and glycolytic metabolic characteristics in intact primary cardiomyocytes. To also test the possible effects of the glutathione precursor, NAC, some cells were treated for 1 h prior to analyses of cellular energetics. In *Grx2-/-* cardiomyocytes, resting and ATP-turnover dependent oxygen consumption rates (OCRs) were abnormally low (Fig. 6A and D). However there were no significant differences in leak respiration or in maximal or spare respiratory capacities (Fig. 6B, C and E). Treating with NAC did not improve respiration in *Grx2-/-* cells compared to treated WT cells in any of the tested conditions. We then probed the metabolic flexibility of the cardiomyocytes through the combined analyses of OCRs and extracellular acidification rates (ECARs). Results clearly demonstrate profoundly limited metabolic flexibility of *Grx2-/-* cells, both in the absence and presence of NAC (Fig. 6F).

2.8. GRX2 transcript expression correlates with key mitochondrial genes in human heart and inversely correlates with adverse heart pathologies

To examine the potential role of GRX2 in the human heart we first examined the level of *GRX2* transcript expression across the tissue samples from the GTEx consortium (GTEx, 2015). *GRX2* transcript levels were expressed at highest levels in the brain, heart (Fig. 7A and Supp. Fig. 2A) and testis (not shown), and demonstrated a wide range of expression levels across the human left ventricle heart samples (Supp. Fig. 2B). Using GTEx left ventricle heart transcriptome data downloaded from the GeneNetwork program (http://www.genenetwork.org), we then performed a gene ontology slim term cellular component analysis of the top 1000 genes that correlated with *GRX2* and found 195 genes classified as components of the mitochondrion (Fig. 7B). Notably, *GRX2* transcript expression was positively correlated to a large sampling of mitochondrial-related genes (Fig. 7C and Supp. Fig. 3). We then grouped GTEx left ventricle tissue samples into those that expressed the highest and lowest levels of *GRX2* transcripts (each n = 50) (Fig. 8A), and compared histopathological phenotypes. Using available images of left ventricle H & E histology sections and pathologist's notes from the GTEx Portal, there was substantially greater evidence of moderate to extensive fibrosis, hypertrophy and infarct in the group of 50 samples with low *GRX2* expression *vs* those with high *GRX2* expression (Fig. 8B and C). These results are consistent and complement our key findings from the *Grx2-/-* mouse model by demonstrating an inverse relationship between *GRX2* expression and cardiac disease in humans.

3. Discussion

Mitochondrial glutathione redox balance in the heart is important to support the exceptionally high rates of oxidative reactions while minimizing oxidative stress. In the present study, we investigated mechanisms impacted by Grx2 deficiency in intact primary cardiomyocytes and permeabilized *ex vivo* cardiac myofibers in mice, and

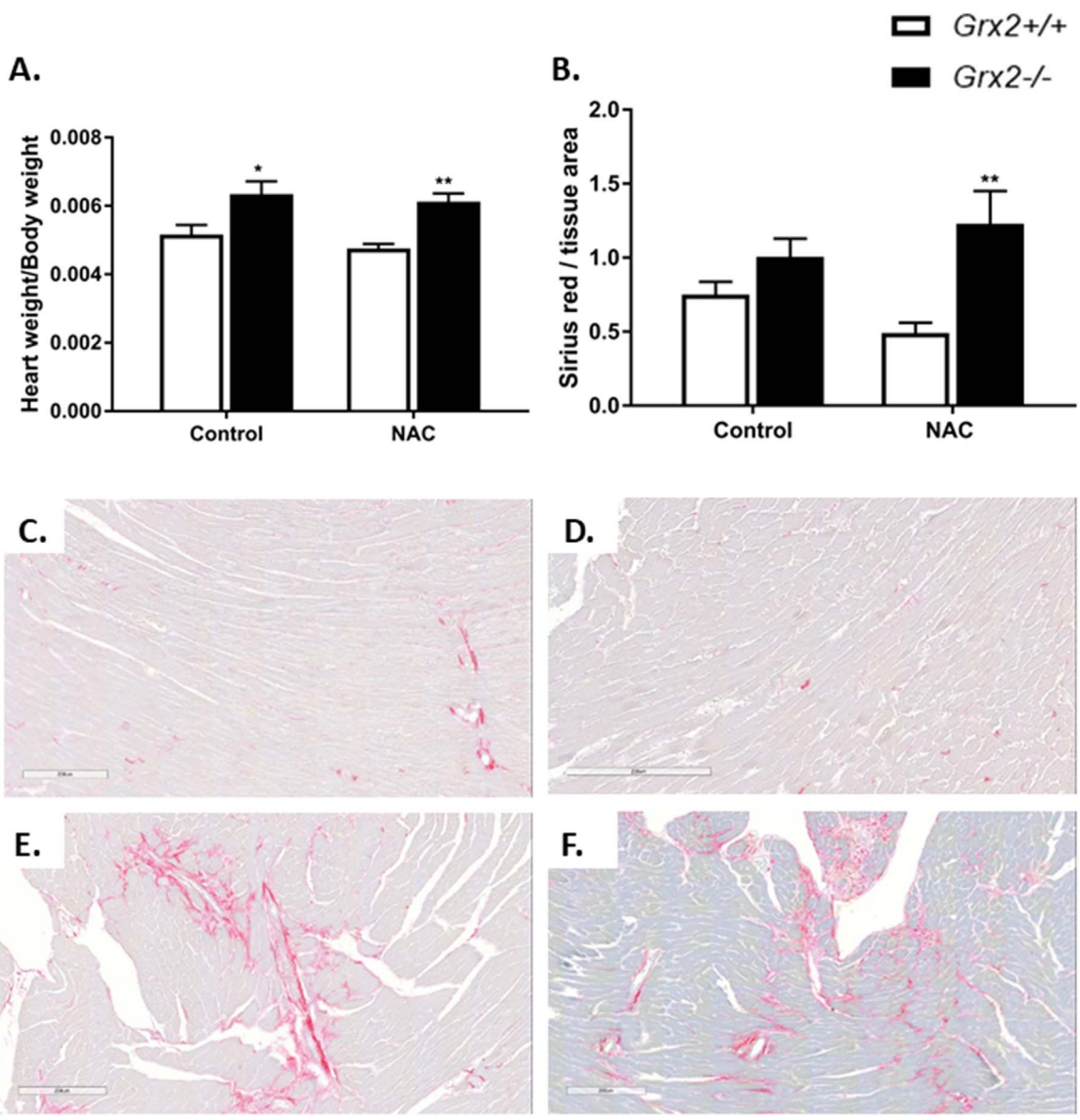

Fig. 3. *Cardiac hypertrophy and fibrosis analysis*. (A) Weight of hearts normalized to body weight. (B) Fibrosis quantification was done using Imagescope software. Images of left ventricle in (C) untreated WT mice, (D) NAC treated WT mice, (E) untreated *Grx2-/-* mice and (F) NAC treated *Grx2-/-* mice. N = 3–6, data are represented as mean ± SEM. Two-way ANOVA with Tukey post-hoc test; $*p < 0.05$, $**p < 0.01$. Scale bar for all images: 200 μm.

complimented this with studies into the GTEx human data resource database and associated tissue bank. We also examined the effects of mouse *in vivo* and *in vitro* supplementation of the glutathione precursor, NAC. We hypothesized that NAC would increase glutathione redox and thereby mitigate, at least in part, the functional impairments. This was based on previous findings showing that oxidative stress is important in establishing cardiac remodeling and fibrosis, leading to a failing myocardium and thus heart failure [13,23,24]. Uncontrolled oxidative stress increases cardiac collagen type I and IV, fibronectin and impairs cardiac contractility [25]. Previous studies also showed that NAC can protect against oxidative stress-mediated cardiac dysfunction. Moreover, in a heart failure rat model, the glutathione content of the left ventricle was shown to be decreased and treatment with NAC was able to lower oxidative stress, the expression of the pro-inflammatory cytokine tumor necrosis factor alpha (TNF-α) and its receptor, and to restore cardiac function and damage [26]. In this context it is important to note that while we previously observed clearly lower glutathione redox in isolated mitochondria of in *Grx2-/-* mice, there is no evidence of increased ROS production or oxidative stress in the heart of these mice [11]. Thus we anticipated that NAC would mitigate dysfunction through the restoration of glutathione redox in *Grx2-/-* mice.

Echocardiography showed that NAC did not affect cardiac functions in WT mice, and more importantly did not abolish cardiac hypertrophy in *Grx2-/-* mice. Moreover, NAC treatment of *Grx2-/-* mice was associated with a possible mitral valve abnormality and diastolic dysfunction. NAC treated *Grx2-/-* mice had a decreased velocity ratio of the early filling wave (E) to the atrial contraction peak (A). In addition, non-invasive blood pressure measurements show that NAC did not mitigate hypertension in *Grx2-/-* mice. It is possible that in the absence of Grx2, NAC treatment causes glutathionylation of key cardiac proteins leading to slower kinetics and increased calcium sensitivity, which in turn can result in sarcomere dysfunction, cardiac hypertrophy and hypertension [27].

It appears that the absence of Grx2 in mice causes profound defects in mitochondrial function that are intransigent to glutathione precursor supplementation. This may be why our results differ from those in which diastolic dysfunction and hypertrophy in familial hypertrophic cardiomyopathy were reversed by NAC [27,28].

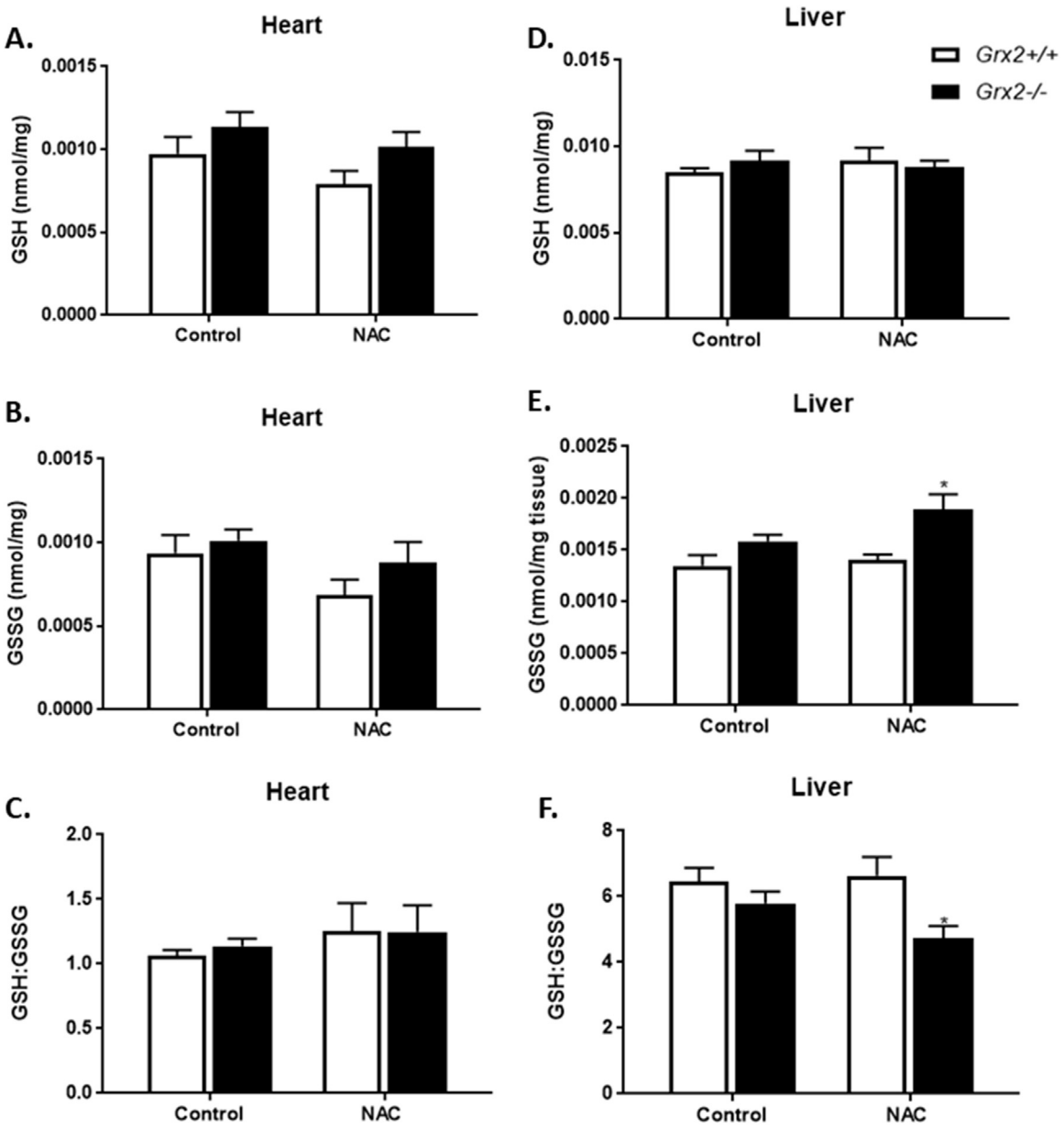

Fig. 4. *NAC treatment alters glutathione redox in the liver but not the heart of Grx2-/- mice.* Measurements of: (A) GSH, (B) GSSG and (C) GSH:GSSG ratio in the heart; (D) GSH, (E) GSSG and (F) GSH:GSSG ratio in the liver. N = 6, data are represented as mean ± SEM. Two-way ANOVA with Tukey post-hoc test.

Furthermore, given the importance of mitochondrial structure to mitochondrial functions, we investigated characteristics of mitochondrial OXPHOS in left ventricle myofibers in which mitochondria remain intact. We observed impaired maximal respiration, and no effect of NAC treatment in *Grx2-/-*. Surprisingly NAC lowered oxygen consumption in WT tissue, without rescuing *Grx2-/-* mice respiration. In a previous study we showed that the reducing agent DTT restored respiration in isolated mitochondria [11]. In the current study, we tested the effects of DTT in intact cardiac myofibers, and indeed we were able to rescue maximal respiration in *Grx2-/-* cardiac myofibers. DTT is a powerful reducing agent that reduces the cellular environment and induces protein deglutathionylation. These findings are consistent with the possibility that in the absence of Grx2 an oxidized environment results in protein glutathionylation (a reversible redox sensitive post-translational modification), and that DTT reduces and reactivates the proteins. Glutathionylation in mitochondria can be enzymatically mediated by Grx2 [16–20]. Disrupted mitochondrial glutathionylation of complex I and ATP synthase can lead to cardiac dysfunction, consistent with the importance of mitochondrial glutathione redox to heart function [21,22].

In a murine model of heart failure, NAC attenuated cardiac remodeling and fibrosis and accelerated wound healing, and had beneficial effects in acute bronchiolitis and congenital heart defects [29,30]. To the contrary, our fibrosis analyses demonstrated higher inflammation in heart tissues from *Grx2-/-* mice treated with NAC compared to other groups. These results further indicate that NAC exacerbates cellular redox in *Grx2-/-*. Interestingly, a recent study in humans showed that NAC was ineffective in treating idiopathic pulmonary fibrosis [31].

In our model, cardiac GSH, GSSG and GSH:GSSG levels were unchanged by *in vivo* NAC treatment. We thus assessed levels in the liver and found increased levels of GSSG and a decrease in GSH:GSSG ratio in treated *Grx2-/-* mice. Many studies in experimental animals and in humans have shown that NAC can increase, decrease or not change glutathione levels. Along with these effects, there is a strong evidence to support the notion that NAC is only beneficial in increasing glutathione levels when GSH levels are depleted in the target tissue [35–40]. This is

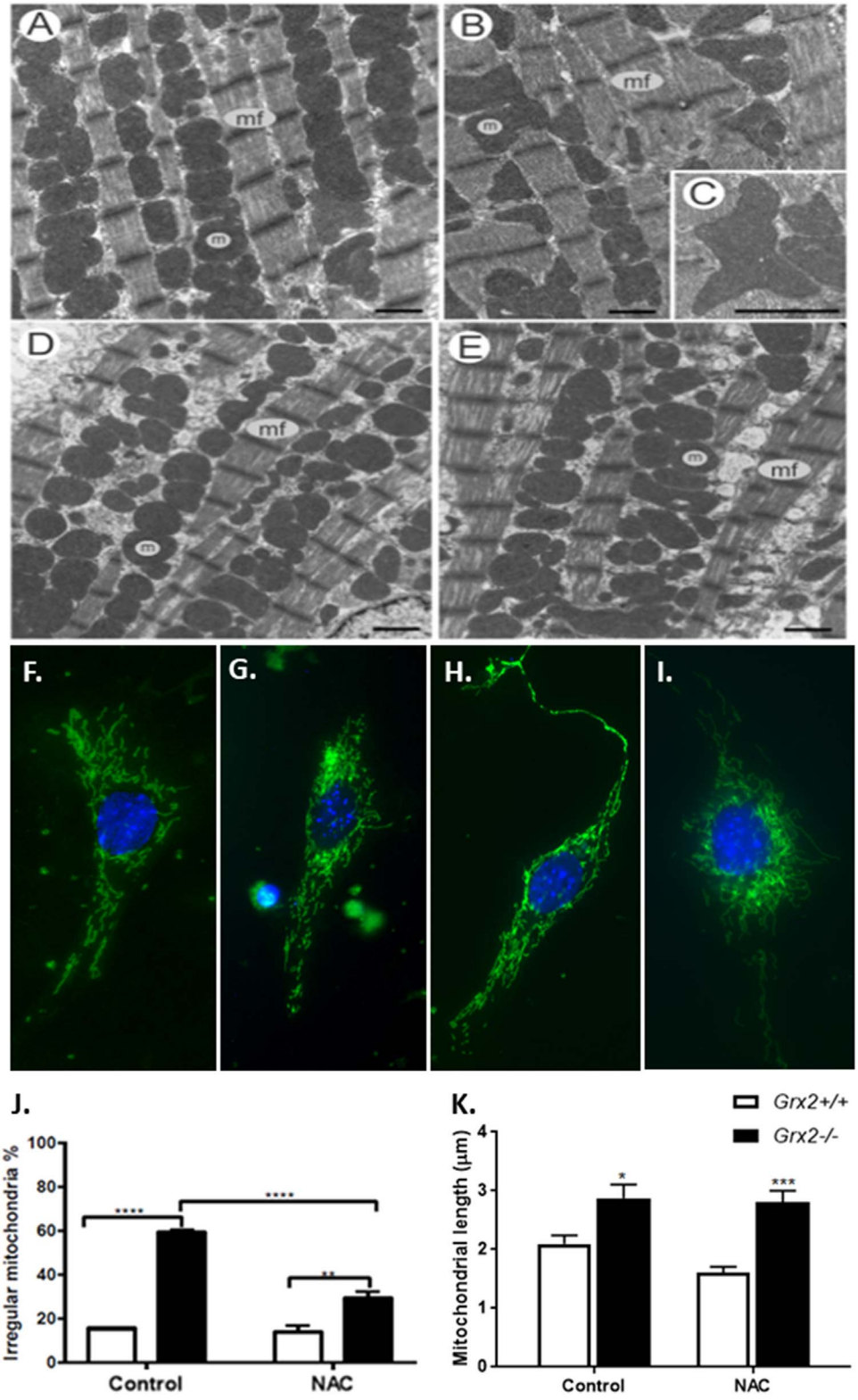

Fig. 5. Abnormal mitochondrial ultrastructural in the myocytes of mouse heart accompanied by mitochondrial tubulation in neonatal cardiomyocytes. (A) Untreated *Grx2*+/+ and (B) *Grx2*-/- hearts. (C) Larger magnification showing irregular mitochondria in *Grx2*-/- heart. (D) NAC treated *Grx2*+/+ and (E) *Grx2*-/- hearts. m; mitochondria, mf; myofibrils. Scale bar for EM images: 1 μm. (F) Untreated *Grx2*+/+, (G) NAC treated *Grx2*+/+, (H) untreated *Grx2*-/-, (I) NAC treated *Grx2*-/-, (J) mitochondrial morphometric analyses and (k) quantification of mitochondrial length. Hoechst dye stains the nucleus (blue) and Tom20 antibody is used to observe the mitochondria (green). N = 15–20, data are represented as mean ± SEM. Two-way ANOVA with Tukey post-hoc test; $*p < 0.05$, $***p < 0.001$. Scale bar for IF images: 200 μm. (For interpretation of the references to color in this figure legend, the reader is referred to the web version of this article.)

an important notion since NAC is also consumed as a nutritional supplement [44, 45].

In our analyses of cardiac tissue levels of GSH and GSSG, we found no effect of *Grx2*-/-. This is in contrast to our previous findings in isolated mitochondria from the hearts of *Grx2*-/- and WT mice [11]. Together, our findings are consistent with the conclusion that there is impaired mitochondrial uptake and/or metabolism of glutathione in the absence of Grx2, and further research is needed to investigate this possibility. Traditionally it has been thought that glutathione is transported into the mitochondrial matrix via the oxoglutarate carrier and/or the dicarboxylate carrier [46], but recent research has challenged this [47].

Mitochondrial dynamics is central in both normal physiology and disease states [32,43]. High levels of oxidized glutathione have previously been shown to control mitochondrial fusion [8], and thus we hypothesized that mitochondrial structure would be abnormal in tissue

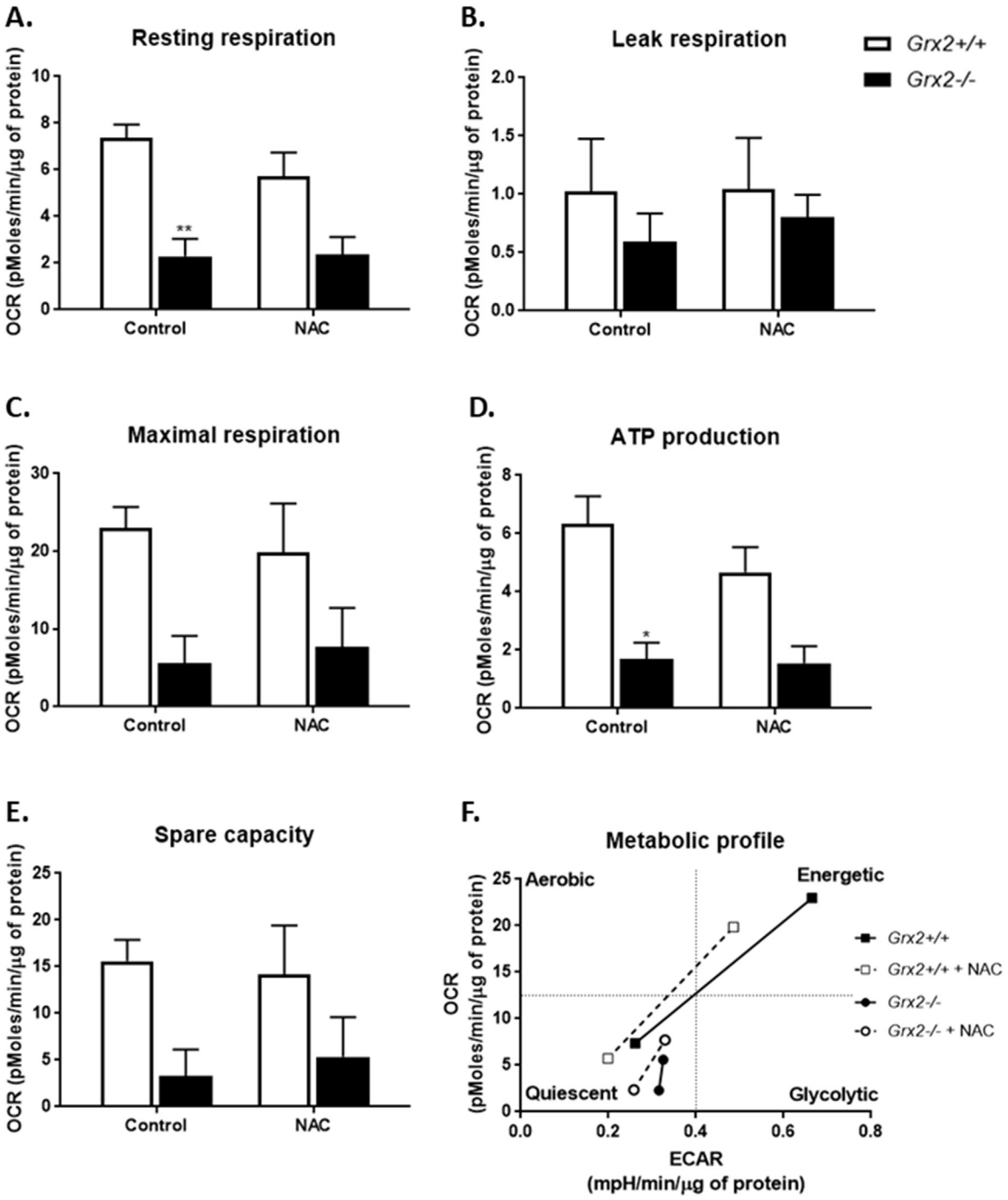

Fig. 6. *Impaired bioenergetics in neonatal cardiomyocytes from Grx2-/- mice.* Mitochondrial respiration was measured using a Seahorse XF 24 analyzer. Oxygen consumption rate (OCR) and extracellular acidification rate (ECAR) were normalized to protein content. (A) Resting respiration, (B) leak respiration, (C) maximal respiration, (D) ATP production, (E) spare capacity and (F) metabolic profile. N = 3, data are represented as mean ± SEM. Two-way ANOVA with Tukey post-hoc test; $*p < 0.05$, $**p < 0.01$.

and primary cell systems in the absence of Grx2. Our electron microscopy analyses demonstrated that mitochondrial ultrastructure in *Grx2-/-* hearts is abnormal, despite normal cristae density. The cross sections of mitochondria revealed unusual angular shapes, which were partially restored to normal ovular-like mitochondrial structures by *in vivo* NAC supplementation. We also assessed mitochondrial length in mouse neonatal primary cardiomyocytes of *Grx2-/-* and WT mice, and demonstrated increased mitochondrial fusion in *Grx2-/-* cells. NAC treatment of the primary cells however did not affect mitochondrial tubulation. While Shutt et al. [8] previously showed that GSH redox regulates mitochondrial fusion, our findings are the first to show that the absence of Grx2 causes mitochondrial elongation in primary cells.

Our analyses of neonatal cardiomyocytes revealed that the absence of Grx2 impacted mitochondrial oxidative phosphorylation as demonstrated by the impaired resting respiration and ATP production in *Grx2-/-* cells. Moreover, contrary to our hypothesis, our results show that in the absence of Grx2, NAC did not ameliorate the respiratory defects; instead it worsened them, consistent with what we observed in cardiac myofibers.

Finally, our findings are the first to show in adult humans that low levels of *GRX2* expression are associated with cardiac disease risk. Through examining GTEx human left ventricle samples, we demonstrate that GRX2 transcript expression is correlated with the expression of various mitochondrial-associated genes. These data agree with the

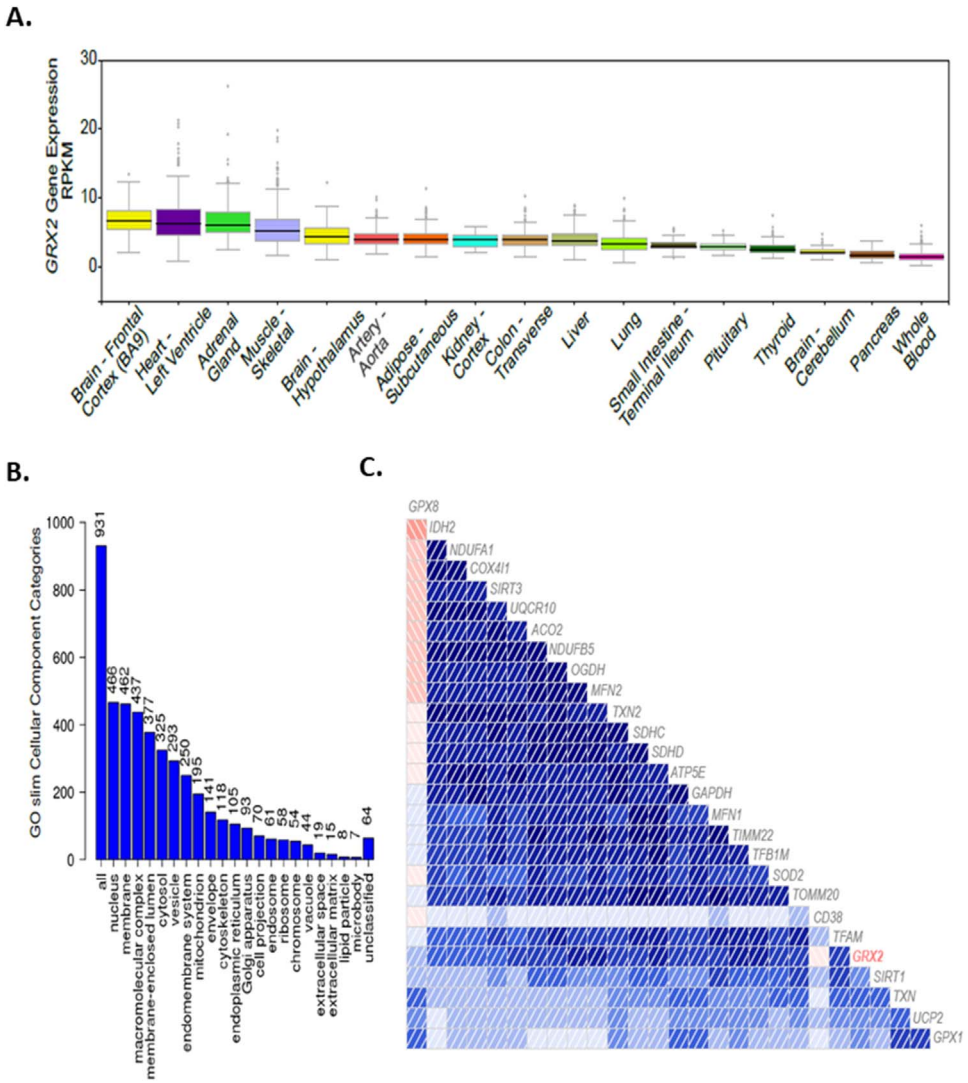

Fig. 7. *Positive correlation between the human GRX2 transcript expression and key mitochondrial genes.* (A) The expression values of *GRX2* (also known as *GLRX2*) in 17 tissue types was plotted using GTEx Analysis Release v6 (dbGaP accession number: phs000424.v6.p1). Expression values were plotted as log(RPKM) (Reads Per Kilobase of transcript per Million mapped reads). Box plots are shown as median and 25th and 75th percentiles; points are displayed as outliers if they are above or below 1.5 times the interquartile range. (B) Gene ontology slim term cellular component category analysis using WebGestalt (WEB-based Gene SeT AnaLysis Toolkit) was performed on the top 1000 genes that were significantly ($P < 0.05$) correlated to GRX2 in data sets derived from the GTEx left ventricle heart tissue transcriptome ($n = 246$; downloaded from the GeneNetwork program at http://www.genenetwork.org). (C) Transcript expression for *GRX2* (shown in red font) were positively correlated with mitochondrial-associated genes using custom-designed data sets derived from the GTEx left ventricle heart tissue transcriptome. As seen on the correlogram, blue correlations are positive (red correlations are negative—intensity of the colors correlates with level of significance). (For interpretation of the references to color in this figure legend, the reader is referred to the web version of this article.)

observed reductions in maximal respiration of intact myofibers from the left ventricle of *Grx2-/-* mice. Notably, consistent with the hypertrophy and fibrosis in *Grx2-/-* mouse hearts, we report moderate/extensive fibrosis, hypertrophy and infarct in human heart samples having low *vs* high expression of GRX2 transcripts. These results support the idea that GRX2 has a cardioprotective role; indeed this would be consistent with the finding of an attenuation of cardiac injury in Grx2 transgenic mice treated with the cardiotoxin, doxorubicin [41]. Thus, these findings clearly emphasize the potential role of GRX2 in protecting against left ventricle pathologies in adult humans.

Altogether, our study is the first to show that Grx2 plays a key role in the control of cellular oxidative and glycolytic functions in cardiomyocytes; that Grx2 is essential for normal mitochondrial dynamics and morphology in cardiomyocytes and heart tissue in mice and humans, and that the GSH precursor, NAC, does not improve mitochondrial energetics or dynamics in mouse *in vitro* or *in vivo* systems. The impact of Grx2 deficiency on the transport of glutathione into mitochondria requires further investigation. Future research into the impact and potential therapeutic implications of *GRX2* in human heart disease is warranted.

4. Methods

4.1. Animals

All experimental procedures involving mice were conducted according to the guidelines and principles of the Canadian Council of Animal Care and after the approval of the Animal Care Committee of the University of Ottawa. In this study, male C57BL/6 mice wild type (WT) and Grx2 whole body knock-out (*Grx2-/-*) were used. Grx2 knock-out was confirmed by PCR before experimentation. All mice were housed in an environment in which temperature, humidity and light cycles (06:00–18:00 h) were controlled.

4.2. Primary cardiomyocyte isolation

Primary cultures of cardiomyocytes were prepared from 1 to 3 day old WT and *Grx2-/-* pups. Each preparation required 15–17 hearts, which were isolated and digested for 10 min, 3–4 times, in Joklik's modified Eagle's medium (M0518-10 × 1L; Sigma-Aldrich) containing 0.1% collagenase (C-2139; Sigma-Aldrich). Enzymatic digestion was stopped with fetal bovine serum (FBS; A12617DJ; Invitrogen), and the undigested tissue was removed by filtration through nylon mesh (pore size, 100 μm). Cardiomyocytes were purified by two pre-platings of 30 min each to remove residual non-myocytes by differential adhesion. Cardiomyocytes were then plated at 120–135 × 10^4 cells/well in a 24-

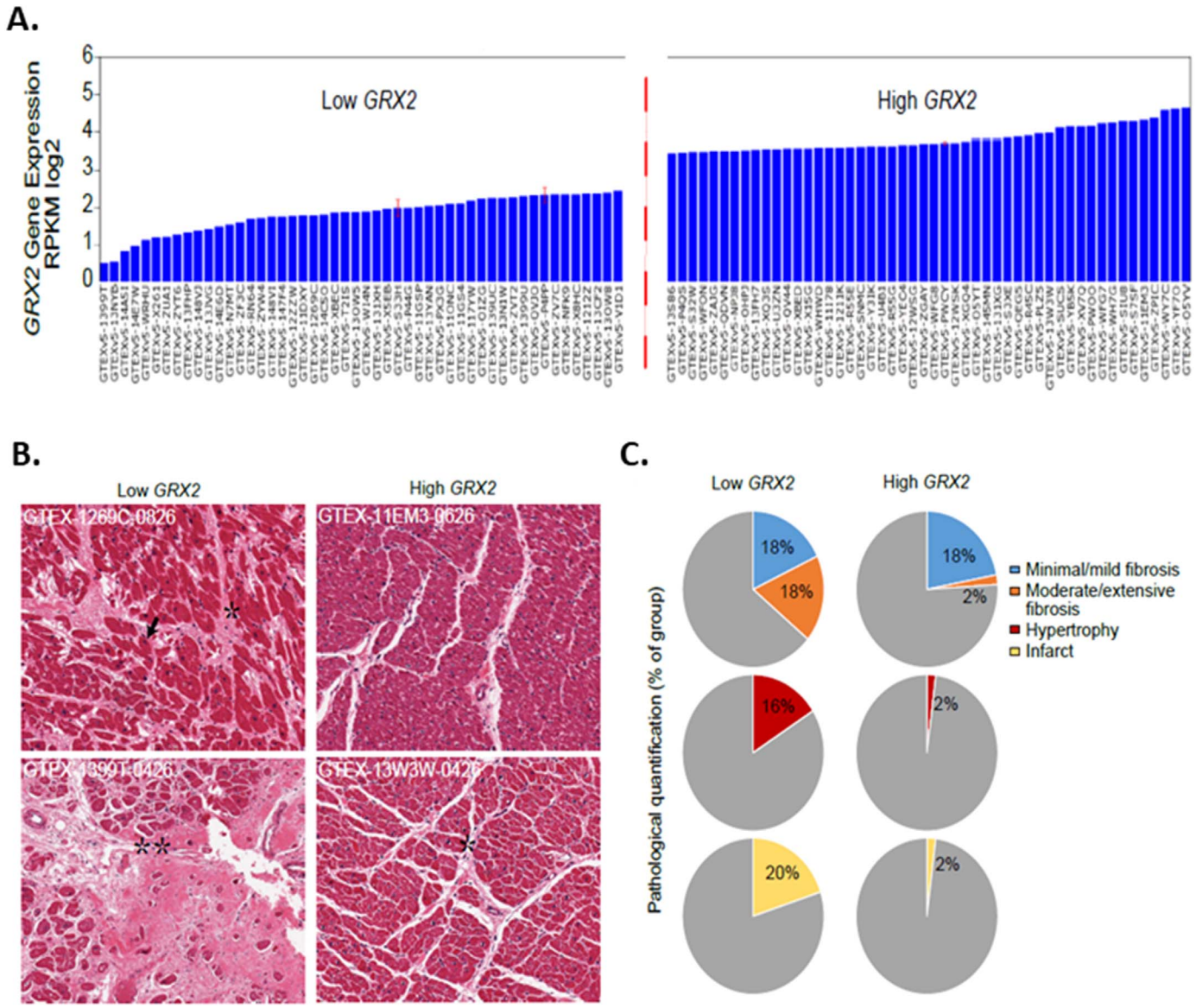

Fig. 8. *Low GRX2 expression in humans is associated with extensive fibrosis, hypertrophy and infarct.* (A) *GRX2* transcript expression data from GTEx left ventricle tissues samples were downloaded from the GeneNetwork program as RPKM log2 values and grouped into those that expressed the highest and lowest levels of *GRX2* transcripts (top n = 50 per group). (B) Representative images for the GTEx left ventricle H & E histology sections for high and low *GRX2* groups (Arrow: hypertrophy; *: fibrosis; **: infarct). Images were downloaded from the GTEx Portal (C) Corresponding pathological notes for all 50 GTEx left ventricle heart samples in the high or low *GRX2* groups were downloaded from the GTEx Portal and quantified to summarize evidence for extensive fibrosis, hypertrophy and infarct.

well plate. Cells were cultured for 16–24 h in Dulbecco's modified Eagle's medium (DMEM; Life Technologies) containing 10% FBS. The following day, the medium was exchanged for serum-free hormonally defined medium (SFHD).

4.3. Bioenergetic determinations of primary cardiomyocytes

Neonatal cardiomyocytes were washed and SFHD media was replaced with Seahorse medium (bicarbonate-free DMEM, 5 mM D-glucose, 4 mM L-glutamine, 1 mM sodium pyruvate; pH 7.4) and incubated in a non-CO_2 incubator at 37 °C for 30 min. The assay cartridge was hydrated with XF calibrant solution one day prior to experiment and left at 37 °C overnight. Oxygen consumption rate (OCR) and extracellular acidification rate (ECAR) measurements were determined using a Seahorse XF24 Extracellular Flux Analyzer (Seahorse Bioscience, Agilent Technologies). Calibration was conducted prior to collection of data. Leak and maximal respiration were measured after injection of 2 μM oligomycin and 1 μM FCCP, respectively (Sigma-Aldrich). Non-mitochondrial respiration was measured after injection of 1 μM antimycin A (Sigma-Aldrich). Following the experiment, cardiomyocytes were lysed with 50 μL of 0.5 M NaOH to conduct protein quantification determination (Bradford assay). Rates were normalized to protein content in each well.

4.4. In vivo NAC supplementation studies

Mice were fed *ad libitum* a standard diet (44.2% carbohydrate, 6.2% fat, 18.6% crude protein; diet T.2018, Harlan Teklad, Indianapolis). Mice were divided into 4 groups (6mice/group): WT untreated, *Grx2-/-* untreated, WT NAC treated and *Grx2-/-* NAC treated. NAC (Sigma-Aldrich, US) was administered to the mice in their drinking water in a dose of 1 g/kg/day from 5 to 11 weeks of age. Previous work established that cardiac hypertrophy develops between 9 and 10 weeks of age [11]. Body weights and food intake were monitored weekly and NAC dosage was adjusted accordingly. Experiments were performed at 12 weeks of age, when body weight was measured in addition to the

weights of the hearts, kidneys, liver, interscapular brown adipose tissue, epididymal white adipose tissue and hindlimb muscles.

4.5. Echocardiography analyses

For echocardiography measurements, a VEVO 2100 system (Visual Sonics, Amsterdam) with a 30-MHz linear array transducer was used. Mice were anesthetized (2.0% isoflurane, 80 ml/min 100% O_2); their anterior chests were shaved and pre-warmed transmission gel was applied. Parasternal long-axis view, short-axis view, two dimensional guided M-mode and Pulsed-Wave Doppler (PWD) images were recorded. Images were analyzed using the VEVO 2100 analysis software.

4.6. Blood pressure determinations

The non-invasive blood pressure analyzer for mice BP-2000 Blood Pressure Analysis System (Visitech Systems; Apex, NC) was used to determine systolic and diastolic blood pressure. At 10 weeks of age, restrained mice were placed on the pre-warmed platform (30 °C) and tails were inserted into the tail cuffs. Measurements were taken between 7:00 and 9:00 a.m. daily for 5 consecutive days. At each session, mice were acclimatized to the system for 10 min before the 20 min measurement period.

4.7. Analyses of cardiac muscle mitochondrial ultrastructure

Left ventricle fragments were dissected, and small pieces of the left ventricle were fixed in 2.5% glutaraldehyde in 0.1 M cacodylate buffer (pH 7.5) at 4 °C. Fixed pieces were washed in cacodylate buffer, post-fixed in 2% OsO_4 in 0.1 M cacodylate buffer for 1 h, rinsed in 0.1 M cacodylate buffer and distilled water, dehydrated in an ethanol series and embedded in Spurr's resin. Resin blocks were sectioned using an ultramicrotome (EM UC6; Leica Microsystems, Canada) using a diamond knife. Ultra-thin sections were mounted on copper grids coated with formvar film. Sections were stained with 2% alcoholic uranyl acetate and Reynold's lead citrate. Stained sections were examined with a transmission electron microscope (JEOL 1230; JEOL Ltd., Tokyo). Morphometric analyses were completed on 178 images (39 images *Grx2*+/+ untreated, 37 images *Grx2*-/- untreated, 42 images *Grx2*+/+ NAC treated and 60 images *Grx2*-/- NAC treated). In total 6833 mitochondria were analyzed and classified. Irregular mitochondria were defined as weirdly branched, tortuous and non-ovular.

4.8. Cardiac fibrosis analysis

Mouse hearts were placed in 10% formalin and then in 70% ethanol prior to paraffin embedding. At the vertical midpoint, 4 μm transverse sections were obtained and stained with Sirius Red, to stain Type 1 and Type 3 collagen fibers. Fibrosis was assessed using Imagescope software (Leica Biosystems) in which stained fibers were quantified and normalized to the tissue area.

4.9. Cardiac and hepatic GSH:GSSG determinations

After isolation, heart left ventricle and liver tissues were weighed and put directly into homogenization bead tubes containing 125 mM sucrose, 5 mM TRIS, 1.5 mM EDTA, 0.5%TFA and 0.5%MPA in mobile phase. A MagNA lyser (Roche, USA) was used to homogenize the tissue. Then samples were spun at 14000xg at 4 °C for 20 min. Supernatants were collected and either analyzed directly using an Agilent HPLC system equipped with a Pursuit C_{18} column (150 ×4.6 mm, 5 μm; Agilent Technologies) operating at a flow rate of 1 ml/min or stored at −80 °C for later analysis. The mobile phase consisted of 0.09% trifluoroacetic acid diluted in ddH2O and mixed with HPLC-grade methanol in a 90:10 ratio. Standard solutions were used to estimate the retention times for GSH and GSSG. Using Agilent Chemstation software, absolute amounts of GSH and GSSG were acquired by integrating the area under the corresponding peaks, and values were calculated from standard curves.

4.10. High resolution respirometry of permeabilized cardiac myofibers

In separate cohorts of mice, the left ventricle was removed and fibers were permeabilized with 50 μg/ml of saponin. Characteristics of mitochondrial respiration were determined in duplicate and at 37 °C (0.5 mM ethylene glycol tetraacetic acid, 3 mM $MgCl_26H_2O$, 20 mM taurine, 10 mM KH_2PO_4, 20 mM N-2-hydroxyethylpiperazine-N-2-ethane sulfonic acid, 110 mM D-sucrose, 0.1% bovine serum albumin and 60 mM lactobionic acid; pH 7.1) using the Oxygraph-2k (Oroboros, Austria). To assess adenylate-free leak respiration and complex I driven respiration, malate (2 mM), pyruvate (5 mM) and glutamate (10 mM) were added to the incubation medium followed by addition of adenosine diphosphate and Mg^{2+} (5 mM). To assess the maximum oxidative phosphorylation capacity (Complex I and II), succinate (10 mM) and ADP (5 mM) were added. Leak supported respiration was assessed by adding oligomycin (2 μg/ml). By adding complex III inhibitor antimycin A (2.5 μM), non-mitochondrial oxygen consumption was determined. N,N,N′,N′-Tetramethyl-p-phenylenediamine (TMPD) (0.5 mM), ascorbate (2 mM) and sodium azide (15 mM) were subsequently added to assess complex IV activity. All values were corrected for residual non-mitochondrial oxygen consumption.

4.11. Mitochondrial fusion characteristics in primary cardiomyocytes

Isolated neonatal cardiomyocytes were washed with PBS and fixed with 4% PFA for 20 min. Cells were rinsed, then permeabilized in PBS with 0.1% Tween-20 for 30 min at room temperature. An incubation of 30 min in PBS with 1% BSA and 0.1% Triton X-100 solution was used to block non-specific binding. Using the same buffer, cells were incubated with anti-Tom20 (Santa Cruz 11415) and with Oregon green 488 antibodies (Thermo Fisher O-11038) for 1 h each at room temperature. Nuclear staining was performed with Hoechst (Thermo Fisher H1399). The concentration of the antibodies was 1:100. Cells were imaged using Zeiss AxioImager M2 microscope (Carl Zeiss, USA). Mitochondrial length was assessed using Image J software (NIH, USA).

4.12. Identification of transcript correlations in GTEx human tissue data sets

Human left ventricle heart microarray data (Affymetrix Human Gene 1.1 ST Array) were analyzed for correlations between *GRX2* (*GLRX2*) transcript expression and mitochondrial-associated genes using the GeneNetwork program. Raw microarray data are also publicly available on Gene Expression Omnibus (GEO; http: //www.ncbi.nlm.nih.gov/geo) under the accession number GSE45878 (GTEx, 2015) and on GeneNetwork (www.genenetwork.org).

4.13. Statistical analyses

All data are represented as mean ± SEM. Statistical analyses were performed using GraphPad Prism 6 (GraphPad Prism, La Jolla, CA, USA). Data were analyzed by two-way repeated measures analysis of variance (ANOVA) with Bonferroni or Tukey post-hoc tests, as indicated. $P < 0.05$ was considered significant.

4.14. Data availability

GTEx expression data for *GRX2* (*GLRX2*) is available here: http://www.gtexportal.org/home/gene/GLRX2. GTEx histology images and pathological notes are available using the GTEx Histology Image Viewer: https://gtexportal.org/home/histologyPage. The data were obtained from the GTEx Portal on 05/17.

Acknowledgments

Authors are grateful for the help of the members of the University of Ottawa Pathology Laboratory in for their histological work. This research was supported by the Canadian Institute of Health Research (FDN 143278) and by Heart and Stroke Foundation of Canada (NA7301). Georges N. Kanaan was supported by the University of Ottawa PhD full admission scholarship.

Conflict of interest

The authors have no conflict of interest to declare.

Author contributions

GNK and MEH conceived the idea for the project. GNK conducted most of the experiments and analyzed most of the results. MN conceived and coordinated the neonatal cardiomyocyte isolations and the echocardiographic determinations while LG and WM conducted the analyses. AR prepared samples for electron microscopy and collected the micrographs. BI helped in fibrosis analysis and Seahorse bioenergetics analyses of cardiomyocytes. DP helped with HPLC analyses. JYX helped with animal handling and genotyping. PM and KM acquired the human data from GTEx consortium and analyzed the data. JV conducted the histopathological analysis of the human left ventricles. GNK and MEH wrote the paper and all authors reviewed and approved it.

Appendix A. Supplementary material

Supplementary data associated with this article can be found in the online version at http://dx.doi.org/10.1016/j.redox.2017.10.019.

References

[1] F.Q. Schafer, G.R. Buettner, Redox environment of the cell as viewed through the redox state of the glutathione disulfide/glutathione couple, Free Radic. Biol. Med. 30 (2001) 1191–1212.
[2] P. Kovacic, R.S. Pozos, R. Somanathan, N. Shangari, P.J. O'Brien, Mechanism of mitochondrial uncouplers, inhibitors, and toxins: focus on electron transfer, free radicals, and structure–activity relationships, Curr. Med. Chem. 12 (2005) 2601–2623.
[3] L.A. Ridnour, J.S. Isenberg, M.G. Espey, D.D. Thomas, D.D. Roberts, D.A. Wink, Nitric oxide regulates angiogenesis through a functional switch involving thrombospondin-1, Proc. Nat. Acad. Sci. USA 102 (2005) 13147–13152.
[4] G. Bartosz, Reactive oxygen species: destroyers or messengers? Biochem. Pharmacol. 77 (2009) 1303–1315.
[5] J.D. Lambeth, NOX enzymes and the biology of reactive oxygen, Nat. Rev. Immunol. 4 (2004) 181–189.
[6] J. Butler, Thermodynamic considerations of free radical reactions, in: C.J. Rhodes (Ed.), Toxicology of the Human Environment, Taylor and Francis, London, 2000, pp. 437–453.
[7] W. Dröge, Free radicals in the physiological control of cell function, Physiol. Rev. 82 (2002) 47–95.
[8] T. Shutt, M. Geoffrion, R. Milne, H.M. McBride, The intracellular redox state is a core determinant of mitochondrial fusion, EMBO Rep. 13 (2012) 909–915.
[9] C.M. Koehler, K. Beverly, E.P. Leverich, Redox pathways in the mitochondrion, Antioxid. Redox Signal. 8 (2006) 813–822.
[10] C. Jacob, I. Knight, P.G. Winyard, Aspects of the biological redox chemistry of cysteine: from simple redox responses to sophisticated signalling pathways, J. Biol. Chem. 387 (2006) 1385–1397.
[11] R.J. Mailloux, J.Y. Xuan, S. McBride, W. Maharsy, S. Thorn, C.E. Holterman, C.R.J. Kennedy, P. Rippstein, R. deKemp, J. DaSilva, M. Nemer, M. Lou, M.E. Harper, Glutaredoxin-2 is required to control oxidative phosphorylation in cardiac muscle by mediating deglutathionylation reactions, J. Biol. Chem. 289 (21) (2014) 14812–14828.
[12] B.H. Lorell, B.A. Carabello, Left ventricular hypertrophy, Circulation 102 (2000) 470–479.
[13] M.G. Rosca, C.L. Hoppel, Mitochondria in heart failure, Cardiovasc. Res. 88 (2010) 40–50.
[14] M. Lundberg, C. Johansson, J. Chandra, M. Enoksson, G. Jacobsson, J. Ljung, M. Johansson, A. Holmgren, Cloning and expression of a novel human glutaredoxin (Grx2) with mitochondrial and nuclear isoforms, J. Biol. Chem. 276 (2001) 26269–26275.
[15] R.J. Mailloux, J.Y. Xuan, B. Beauchamp, L. Jui, M. Lou, M.E. Harper, Glutaredoxin-2 is required to control proton leak through uncoupling protein-3, J. Biol. Chem. 288 (2013) 8365–8379.
[16] J.J. Mieyal, M.M. Gallogly, S. Qanungo, E.A. Sabens, M.D. Shelton, Molecular mechanisms and clinical implications of reversible protein S-glutathionylation, Antioxid. Redox Signal. 10 (11) (2008) 1941–1988.
[17] C.L. Grek, J. Zhang, Y. Manevich, D.M. Townsend, K.D. Tew, Causes and consequences of cysteine S-glutathionylation, J. Biol. Chem. 288 (37) (2013) 26497–26504.
[18] S.M. Beer, E.R. Taylor, S.E. Brown, C.C. Dahm, N.J. Costa, M.J. Runswick, M.P. Murphy, Glutaredoxin 2 catalyzes the reversible oxidation and glutathionylation of mitochondrial membrane thiol proteins: implications for mitochondrial redox regulation and antioxidant DEFENSE, J. Biol. Chem. 279 (46) (2004) 47939–47951.
[19] R.J. Mailloux, S.L. McBride, M.E. Harper, Unearthing the secrets of mitochondria ROS and glutathione in bioenergetics, Trends Biochem. Sci. 38 (12) (2013) 592–602.
[20] T.R. Hurd, R. Requejo, A. Filipovska, S. Brown, T.A. Prime, A.J. Robinson, I.M. Fearnley, M.P. Murphy, Complex I within oxidatively stressed bovine heart mitochondria is glutathionylated on Cys-531 and Cys-704 of the 75-kDa subunit: potential role of Cys residues in decreasing oxidative damage, J. Biol. Chem. 283 (2008) 24801–24815.
[21] S.B. Wang, D.B. Foster, J. Rucker, B. O'Rourke, D.A. Kass, J.E. Van Eyk, Redox regulation of mitochondrial ATP synthase: implications for cardiac resynchronization therapy, Circ. Res. 109 (2011) 750–757.
[22] C. Passarelli, G. Tozzi, A. Pastore, E. Bertini, F. Piemonte, GSSG-mediated complex I defect in isolated cardiac mitochondria, Int. J. Mol. Med. 26 (2010) 95–99.
[23] H. Tsutsui, T. Ide, S. Kinugawa, Mitochondrial oxidative stress, DNA damage, and heart failure, Antioxid. Redox Signal. 8 (9–10) (2006) 1737–1744, http://dx.doi.org/10.1089/ars.2006.8.1737.
[24] Y.K. Tham, B.C. Bernardo, J.Y.Y. Ooi, K.L. Weeks, J.R. McMullen, Pathophysiology of cardiac hypertrophy and heart failure: signaling pathways and novel therapeutic targets, Arch. Toxicol. 89 (9) (2015) 1401–1438, http://dx.doi.org/10.1007/s00204-015-1477-x.
[25] M. Aragno, R. Mastrocola, G. Alloatti, I. Vercellinatto, P. Bardini, S. Geuna, G. Boccuzzi, Oxidative stress triggers cardiac fibrosis in the heart of diabetic rats, Endocrinology 149 (1) (2008) 380–388, http://dx.doi.org/10.1210/en.2007-0877.
[26] C. Adamy, P. Mulder, L. Khouzami, N. Andrieu-abadie, N. Defer, G. Candiani, F. Pecker, Neutral sphingomyelinase inhibition participates to the benefits of N-acetylcysteine treatment in post-myocardial infarction failing heart rats, J. Mol. Cell. Cardiol. 43 (3) (2007) 344–353, http://dx.doi.org/10.1016/j.yjmcc.2007.06.010.
[27] T. Wilder, D.M. Ryba, D.F. Wieczorek, B.M. Wolska, R.J. Solaro, N-acetylcysteine reverses diastolic dysfunction and hypertrophy in familial hypertrophic cardiomyopathy, Am. J. Physiol. Heart Circ. Physiol. 309 (10) (2015) H1720–H1730, http://dx.doi.org/10.1152/ajpheart.00339.2015.
[28] M.-C. Chaumais, B. Ranchoux, D. Montani, P. Dorfmüller, L. Tu, F. Lecerf, F. Perros, N-acetylcysteine improves established monocrotaline-induced pulmonary hypertension in rats, Respir. Res. 15 (2014) 65, http://dx.doi.org/10.1186/1465-9921-15-65.
[29] B. Giam, P.-Y. Chu, S. Kuruppu, A.I. Smith, D. Horlock, H. Kiriazis, N.W. Rajapakse, N-acetylcysteine attenuates the development of cardiac fibrosis and remodeling in a mouse model of heart failure, Physiol. Rep. 4 (7) (2016), http://dx.doi.org/10.14814/phy2.12757.
[30] M. AlMatar, T. Batool, E.A. Makky, Therapeutic potential of N-acetylcysteine for wound healing, acute bronchiolitis, and congenital heart defects, Curr. Drug Metab. 17 (2) (2016) 156–167.
[31] M. Myllärniemi, R. Kaarteenaho, Pharmacological treatment of idiopathic pulmonary fibrosis - preclinical and clinical studies of pirfenidone, nintedanib, and N-acetylcysteine, Eur. Clin. Respir. J. (2015) 2, http://dx.doi.org/10.3402/ecrj.v2.26385.
[32] M. Picard, O.S. Shirihai, B.J. Gentil, Y. Burelle, Mitochondrial morphology transitions and functions: implications for retrograde signaling? Am. J. Physiol.- Regul., Integr. Comp. Physiol. 304 (2013) R393–R406.
[33] P.H.G.M. Willems, R. Rossignol, C.E.J. Dieteren, M.P. Murphy, W.J.H. Koopman, Redox Homeostasis and Mitochondrial Dynamics, Cell Metab. 22 (2015) 207–218.
[34] Y. Samuni, S. Goldstein, O.M. Dean, M. Berk, The chemistry and biological activities of N-acetylcysteine, Biochim. Biophys. Acta 1830 (8) (2013) 4117–4129, http://dx.doi.org/10.1016/j.bbagen.2013.04.016.
[35] M.B. Forman, D.W. Puett, C.U. Cates, D.E. McCroskey, J.K. Beckman, H.L. Greene, R. Virmani, Glutathione redox pathway and reperfusion injury. Effect of N-acetylcysteine on infarct size and ventricular function, Circulation 78 (1) (1988) 202–213.
[36] H.A. Kleinveld, P.N. Demacker, A.F. Stalenhoef, Failure of N-acetylcysteine to reduce low-density lipoprotein oxidizability in healthy subjects, Eur. J. Clin. Pharmacol. 43 (6) (1992) 639–642.
[37] A. Meyer, R. Buhl, S. Kampf, H. Magnussen, Intravenous N-acetylcysteine and lung glutathione of patients with pulmonary fibrosis and normals, Am. J. Respir. Crit. Care Med. 152 (3) (1995) 1055–1060, http://dx.doi.org/10.1164/ajrccm.152.3.7663783.
[38] A.T. Treweeke, T.J. Winterburn, I. Mackenzie, F. Barrett, C. Barr, G.F. Rushworth, I.L. Megson, N-Acetylcysteine inhibits platelet-monocyte conjugation in patients with type 2 diabetes with depleted intraplatelet glutathione: a randomised controlled trial, Diabetologia 55 (11) (2012) 2920–2928, http://dx.doi.org/10.1007/s00125-012-2685-z.
[39] G.F. Rushworth, I.L. Megson, Existing and potential therapeutic uses for N-acetylcysteine: the need for conversion to intracellular glutathione for antioxidant benefits, Pharmacol. Ther. 141 (2) (2014) 150–159, http://dx.doi.org/10.1016/j.

pharmthera.2013.09.006.
[40] M.M. Lasram, I.B. Dhouib, A. Annabi, S. El Fazaa, N. Gharbi, A review on the possible molecular mechanism of action of N-acetylcysteine against insulin resistance and type-2 diabetes development, Clin. Biochem. 48 (16–17) (2015) 1200–1208, http://dx.doi.org/10.1016/j.clinbiochem.2015.04.017.
[41] N.M. Diotte, Y. Xiong, J. Gao, B.H.L. Chua, Y.-S. Ho, Attenuation of doxorubicin-induced cardiac injury by mitochondrial glutaredoxin 2, Biochim. Biophys. Acta 1793 (2) (2009) 427–438, http://dx.doi.org/10.1016/j.bbamcr.2008.10.014.
[42] H. Wu, Y. Yu, L. David, Y.-S. Ho, M.F. Lou, Glutaredoxin 2 (Grx2) gene deletion induces early onset of age-dependent cataracts in mice, J. Biol. Chem. 289 (52) (2014) 36125–36139, http://dx.doi.org/10.1074/jbc.M114.620047.
[43] P. Mishra, D.C. Chan, Metabolic regulation of mitochondrial dynamics, J. Cell Biol. 212 (4) (2016) 379–387, http://dx.doi.org/10.1083/jcb.20151103.
[44] J. Peake, K. Suzuki, Neutrophil activation, antioxidant supplements and exercise-induced oxidative stress, Exerc. Immunol. Rev. 10 (2004) 129–141.
[45] A. Zembron-Lacny, M. Slowinska-Lisowska, Z. Szygula, K. Witkowski, K. Szyszka, The comparison of antioxidant and hematological properties of N-acetylcysteine and alpha-lipoic acid in physically active males, Physiol. Res. 58 (6) (2009) 855–861.
[46] L.H. Lash, Mitochondrial glutathione in diabetic nephropathy, J. Clin. Med. 4 (7) (2015) 1428–1447, http://dx.doi.org/10.3390/jcm4071428.
[47] L.M. Booty, M.S. King, C. Thangaratnarajah, H. Majd, A.M. James, E.R.S. Kunji, M.P. Murphy, The mitochondrial dicarboxylate and 2-oxoglutarate carriers do not transport glutathione, FEBS Lett. 589 (5) (2015) 621–628, http://dx.doi.org/10.1016/j.febslet.2015.01.027.